Charmless Hadronic Penguin B Decays with BaBar: $B^0(\overline{B}^0) \to \overline{K}^{*0}K^0$ or $\eta'\eta'$

J. William Gary
Department of Physics and Astronomy, University of California, Riverside, CA 92521 USA

Received on 29 October, 2006

Recent results from the BaBar experiment on searches for New Physics using the charmless channels $B^0 \to \overline{K}^{*0}K^0$ and $B^0 \to \eta'\eta'$ are discussed.

Keywords: B mesons; Rare charmless decays

I. INTRODUCTION

The BaBar experiment at SLAC studies e^+e^- annihilations at the $\Upsilon(4S)$ resonance. The $\Upsilon(4S)$ is a clean, copious source of B mesons. The $\Upsilon(4S)$ decays about half the time to $B^0\overline{B}^0$ pairs and the other half of the time to B^+B^- pairs. At the $\Upsilon(4S)$ energy, about 75% of the cross section is $e^+e^- \to q\overline{q}$ ($q = u,d,s,c$) continuum events, with the remaining cross section the $e^+e^- \to \Upsilon(4S) \to B\overline{B}$ events. The large continuum background is reduced by considering the kinematic variables m_{ES} and ΔE, with $\Delta E \equiv E^*_B - E^*_{beam}$ and $m_{ES} \equiv \sqrt{E^{*2}_{beam} - P^{*2}_B}$, where E^*_B and P^*_B are the CM energy and momentum of the B meson candidate (reconstructed in the decay channel of interest) and E^*_{beam} is half the CM energy. For B candidates, m_{ES} is peaked at the B mass and ΔE is peaked at zero, while for continuum events m_{ES} and ΔE do not have any peaking structure. A third key variable to reducing the combinatoric background is the event shape. At the $\Upsilon(4S)$ energy, the B and $\overline{B}$ mesons are produced almost at rest. Thus the event is spherical in momentum space. In contrast, the $e^+e^- \to q\overline{q}$ events are jet-like. A Fisher discriminant based on event shape information is used in conjunction with m_{ES} and ΔE to separate the B meson candidates from the continuum background.

The interest in charmless decays, corresponding to $b \to d$ and $b \to s$ quark transitions, is that they are loop diagrams. These transitions are called "penguin" diagrams. Thus, unlike the much more copious $b \to c$ tree-level transitions, penguin transitions are sensitive to physics beyond the Standard Model through the virtual production of New Physics particles. Among the most important purely hadronic B^0 decays being studied by BaBar are the tree-level $B^0 \to J/\Psi K^0$ decay, and the penguin $B^0 \to \phi K^0$ and $B^0 \to \eta' K^0$ decays. Feynman diagrams for these decays are shown in Fig. 1.

Of central interest to current studies of the B meson are measurements of the time dependent CP asymmetry in B^0 and $\overline{B}^0$ decays to a common final state f, defined by

$$A_f^{CP}(t) = \frac{[\Gamma(B^0 \to f)](t) - [\Gamma(\overline{B}^0 \to f)](t)}{\text{sum}} \quad (1)$$
$$= S_f \sin(\Delta m t) - C_f \cos(\Delta m t) \quad (2)$$

This has the simple form in terms of the sin and cos functions as shown in eq. (2), with Δm the neutral B_d mass difference. For f a CP eigenstate and for decays dominated by a single weak phase, conditions which hold for the processes shown in Fig. 1, the coefficients S_f and C_f are given by $S_f = \eta_f \sin(2\beta)$ and $C_f = 0$, where η_f is the CP eigenvalue ($=\pm1$) and $\sin(2\beta)$ is the phase difference between the $B \to f$ and $B \to \overline{B} \to f$ decay paths. Results for S_f determined from eq. (1) for the three channels shown in Fig. 1 are presented in Fig. 2. The corresponding results for C_f are found to be consistent with zero and thus agree with the Standard Model expectation.

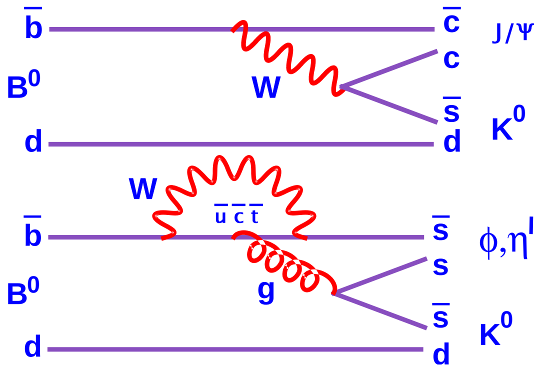

FIG. 1: Feynman diagrams for $B^0 \to J/\Psi K^0$, $B^0 \to \phi K^0$ and $B^0 \to \eta' K^0$.

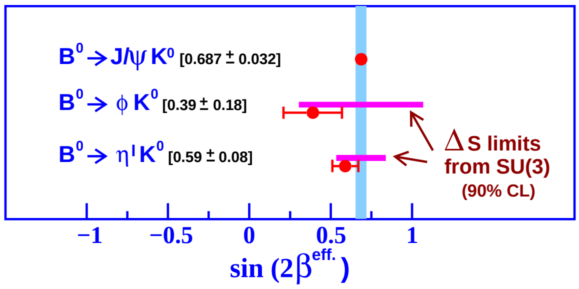

FIG. 2: Effective measurements of $\sin(2\beta)$ from $B^0 \to J/\Psi K^0$, $B^0 \to \phi K^0$ and $B^0 \to \eta' K^0$ decays, as of the ICHEP 2006 meeting.

In contrast to C_f, it is seen that the two loop processes ($B^0 \to \phi K^0$ and $B^0 \to \eta' K^0$) yield results for $\sin(2\beta)$ which are systematically lower than the result from the tree level $J/\Psi K^0$ decay. This deviation is referred to as ΔS, i.e., $\Delta S_f = S_f - \sin(2\beta)$ with $\sin(2\beta) \equiv S_{J/\Psi K^0}$. Deviations $\Delta S \neq 0$ could be caused by New Physics. However, it is also possible that they are caused by sub-dominant Standard Model processes with different weak phases from the dominant diagrams, since this would break the conditions leading to $S_f = \eta_f \sin(2\beta)$. The dominant diagrams are equivalent to those shown in Fig. 1 with, for example, the $\bar{t}$ quark (but not the $\bar{u}$ quark) as the virtual quark in the propagator loop for $B^0 \to \phi K^0$ and $B^0 \to \eta' K^0$. Sub-dominant processes with a different weak phase from the dominant diagrams are referred to as Standard Model pollution. Standard Model pollution to the $B^0 \to \phi K^0$ and $B^0 \to \eta' K^0$ decay modes arise from $b \to u$ transitions corresponding to Fig. 1 with the $\bar{u}$ quark as the virtual quark and to the diagrams shown in Fig. 3.

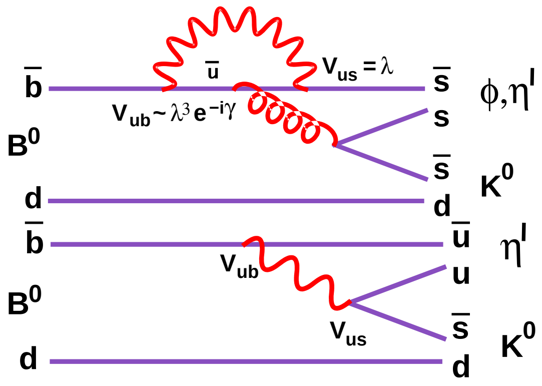

FIG. 3: Diagrams resulting in Standard Model pollution to $B^0 \to \phi K^0$ and $B^0 \to \eta' K^0$.

BaBar recently completed studies of the $B^0 \to \overline{K}^{*0} K^0$ and $B^0 \to \eta'\eta'$. These are published in Refs. [1] and [2], respectively. The principal motivation for studying these two channels is that they can be used to set limits on the $b \to u$ amplitudes (the Standard Model pollution) in $B^0 \to \phi K^0$ and $B^0 \to \eta' K^0$, using the technique based on SU(3) flavor symmetry discussed in Ref. [3]. Consider for example, the Feynman diagrams for $B^0 \to \overline{K}^{*0} K^0$, which are shown in Fig. 4. These are the same as the diagrams for $B^0 \to \phi K^0$ shown in Fig. 1 except that the $\bar{b} \to \bar{s}$ quark transition has been replaced by a $\bar{b} \to \bar{d}$ transition. However, for $B^0 \to \overline{K}^{*0} K^0$, there is no suppression of the $b \to u$ propagator term compared to the $b \to t$ and $b \to c$ terms, unlike the case for $B^0 \to \phi K^0$. The conservative procedure is then to assume that the $B^0 \to \overline{K}^{*0} K^0$ decay rate is dominated by the $b \to u$ term, and to use the observed rate of $B^0 \to \overline{K}^{*0} K^0$ and SU(3) flavor symmetry to set an upper limit on the $b \to u$ amplitude (Standard Model pollution) in $B^0 \to \phi K^0$. Similarly, the $B^0 \to \eta'\eta'$ decay rate is used to set an upper limit on the Standard Model pollution in $B^0 \to \eta' K^0$.

In practice, other charmless, strangeness conserving processes than the two in our study are necessary to set these SU(3) flavor limits on ΔS in $B^0 \to \phi K^0$ and $B^0 \to \eta' K^0$ (see Ref. [3]). However, the two channels of interest for this study have been the limiting factors in this determination. The $B^0 \to \overline{K}^{*0} K^0$ channel has not previously been studied, while the $B^0 \to \eta'\eta'$ was studied with only a substantially smaller data sample.

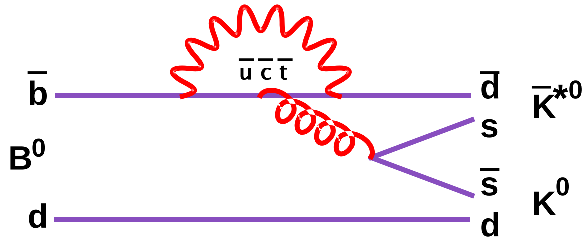

FIG. 4: Feynman diagrams for $B^0 \to \overline{K}^{*0} K^0$.

II. ANALYSIS AND RESULTS

The $\overline{K}^{*0} K^0$ analysis is based on 210 fb^{-1} of data, corresponding to 232 million $B\overline{B}$ pairs. B^0 candidates are reconstructed through $K^{*0} \to K^+\pi^-$ and $K^0 \to K^0_S \to \pi^+\pi^-$. The $\eta'\eta'$ analysis is based on 289 fb^{-1}, corresponding to 324 million $B\overline{B}$ pairs. This corresponds to an increase in event statistics of about a factor of four compared to the previous $\eta'\eta'$ study. The η' is reconstructed in two channels: the $\eta'_{\eta\pi\pi}$ mode (i.e., $\eta' \to \eta\pi^+\pi^-$ with $\eta \to \gamma\gamma$) and the $\eta'_{\rho\gamma}$ mode (i.e., $\eta' \to \rho^0\gamma$ with $\rho^0 \to \pi^+\pi^-$). To reconstruct B^0 candidates, we use $\eta'_{\eta\pi\pi}\eta'_{\eta\pi\pi}$ and $\eta'_{\eta\pi\pi}\eta'_{\rho\gamma}$ combinations. The $\eta'_{\rho\gamma}\eta'_{\rho\gamma}$ combinations are not used because of excessive background.

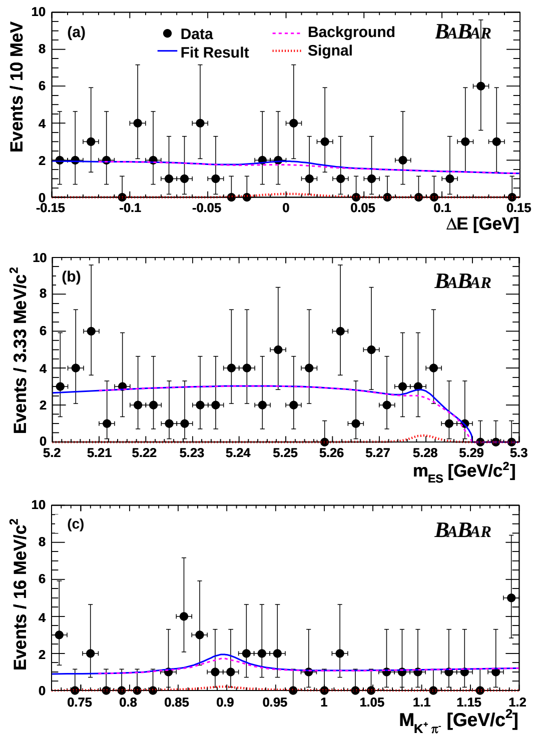

FIG. 5: Projections of the maximum likelihood results in comparison to data for $B^0 \to \overline{K}^{*0} K^0$.

The $\overline{K}^{*0} K^0$ analysis employs particle identification of the K^+ and π^-, based on energy loss measurements in the tracking chambers (dE/dx) and radiation in ring imaging Cherenkov detectors. After cutting on event shape measurements to reduce continuum background, an extended maximum likelihood fit is applied to the ΔE, m_{ES} and $M_{K^+\pi^-}$ distributions, with $M_{K^+\pi^-}$ the invariant mass of the K^{*0} candidate. Projections of the fit results are shown in comparison to the data in Fig. 5. Of the 682 events that survive the preliminary cuts, 660 ± 75 are found to be continuum background and 21^{+74}_{-71} background from $B\overline{B}$ events. The number of $B^0 \to \overline{K}^{*0} K^0$ events is found to be $1.0^{+4.7}_{-3.9}$. The overall detection efficiency is 2.2%. The measured branching fraction is $(0.2^{+0.9}_{-0.8}{}^{+0.1}_{-0.3}) \times 10^{-6}$. We set a 90% confidence level upper limit on the branching fraction of 1.9×10^{-6}. As mentioned above, these are the first results for this channel.

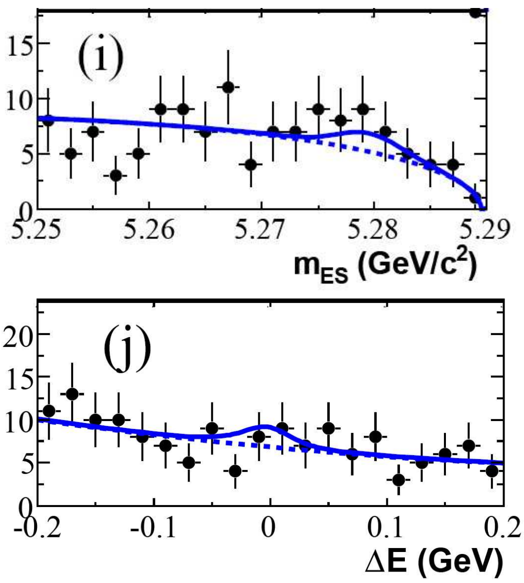

FIG. 6: Projections of the fit results in comparison to data for $B^0 \to \eta'\eta'$.

The extended maximum likelihood fit for the $\eta'\eta'$ analysis is based on more variables: the event shape information, ΔE, m_{ES} and the two η' reconstructed masses. For the $\eta'_{\rho\gamma}$ decay mode, the ρ helicity angle is also included in the fit. The results of the $\eta'\eta'$ fit are given in Table I. The corresponding fit projections are shown in comparison to the data in Fig. 6. The 90% confidence level upper limit we obtain for the branching fraction is 2.4×10^{-6}, a factor of four improvement compared to the previous result.

III. SUMMARY AND CONCLUSIONS

Using the formalism of Ref. [3], we set the following limits on the level of deviation of the effective $\sin(2\beta)$ measurements in $B^0 \to \phi K^0$ and $B^0 \to \eta' K^0$ compared to $B^0 \to J/\Psi K^0$: $\Delta S_{\phi K^0} < 0.38$ and $\Delta S_{\eta' K^0} < 0.15$. The ϕK^0 result is the first for this bound. The $\eta' K^0$ result can be compared to the previous bound of 0.22. The SU(3) bounds we obtain are shown

TABLE I: Results from the extended maximum likelihood fit for $\eta'\eta'$.

Mode	Yield (evts.)	Eff.(%)	$\prod \mathcal{B}_i$ (%)	$S(\sigma)$	$\mathcal{B}(10^{-6}$
$\eta'_{\eta\pi\pi}\eta'_{\eta\pi\pi}$	1^{+2}_{-1}	15.2 ± 1.0	3.1	1.2	$0.8^{+1.3}_{-0.7}$
$\eta'_{\eta\pi\pi}\eta'_{\rho\gamma}$	9^{+7}_{-5}	17.6 ± 0.8	10.3	1.5	$1.2^{+1.1}_{-0.9}$
$\eta'\eta'$				1.8	$1.0^{+0.8}_{-0.6} \pm 0.1$

by the horizontal bars in Fig. 2. The observed ΔS deviations observed for the ϕK^0 and $\eta' K^0$ are seen to be compatible with the $\sin(2\beta)$ result from $J/\Psi K^0$ within these bounds. Therefore, we do not observe evidence for New Physics. BaBar is expected to collect data until the end of 2008 and should have a final data sample of about 1 ab^{-1}. This will result in an increase by about a factor of three in the available number of events compared to the numbers used in the two studies presented here, corresponding to an expected improvement of about 60% in the ΔS bounds based on SU(3) flavor symmetry.

[1] BABAR Collaboration, B. Aubert, et al. Phys. Rev. D **74**, 072008 (2006).
[2] BABAR Collaboration, B. Aubert, et al. Phys. Rev. D **74**, 051106(R) (2006),
[3] Y. Grossman et al., Phys. Rev. D **68**, 015004 (2003).